

A Neural Network-Based Method for Brain Abnormality Detection in MR Images Using Zernike Moments and Geometric Moments

AmirEhsan Lashkari
University of Tehran, School of
Electrical and Computer engineering
Campus No. 2, North Kargar Avenue
P.O. BOX 14395/515 Tehran. I.R. of
IRAN

ABSTRACT

Nowadays, automatic defects detection in *MR* images is very important in many diagnostic and therapeutic applications. Because of high quantity data in *MR* images and blurred boundaries, tumor segmentation and classification is very hard. This paper has introduced one automatic brain tumor detection method to increase the accuracy and yield and decrease the diagnosis time. The goal is classifying the tissues to two classes of normal and abnormal. *MR* images that have been used here are *MR* images from normal and abnormal brain tissues. Here, it is tried to give clear description from brain tissues using *Zernike* Moments, Geometric Moment Invariants, energy, entropy, contrast and some other statistic features such as mean, median, variance, correlation, values of maximum and minimum intensity. It is used from a feature selection method to reduce the feature space too. this method uses from neural network to do this classification. The purpose of this project is to classify the brain tissues to normal and abnormal classes automatically, that saves the radiologist time, increases accuracy and yield of diagnosis.

General Terms

Pattern Recognition, Image Processing, Soft Computation, Artificial Intelligent.

Keywords

Feature extraction, Kernel F-score feature selection, Gabor wavelets, artificial neural network, tumor detection, segmentation, *MR* images.

1. INTRODUCTION

Body is made of many cells. Each cell has specific duty. The cells growth in the body and are divided to reproduce other cells. These divisions are very vital for correct functions of the body. When each cell loses the ability of controlling its growth, these divisions is done with any limitation and tumor emerges. Tumors, their self, are divided to tow classes: benign and malignant. According to a statistical report published by the Central Brain Tumor Registry of the United States (*CBTRUS*), approximately 39,550 people were newly diagnosed with primary benign and primary malignant brain tumors in 2002 [1-3]. Furthermore, in 2000, more than 81,000 people, in the United States alone, were living with a primary malignant brain tumor and 267,000 were living with a primary benign brain tumor. The same report indicates that the incidence rate of primary brain tumors, whether benign or

malignant, is 14 per 100,000, while median age at diagnosis is 57 years [3].

MR imaging technique, because of good ability in showing difference between soft tissues, high resolution, good contrast and noninvasive technique for using no ionization rays is very appropriate. Segmentation is the first step at quantitative analysis of medical images. Medical images analysis field [4, 5, 6], because of indirect and Sophisticate structures are very complicated but interesting. Segmentation methods are very successful on normal tissues [4, 7-12] but it hasn't been done good theoretical and practical segmentation on abnormal tissues yet [4]. Computer aided tumor detection is one of the hardest index in field of abnormal tissue segmentations. There are two important problems. First, automatic tissue measurement is not very easy because of variations in the structures. Intensity distribution of normal tissues is very complicated and exist some overlaps between different types of tissues. Moreover it is probable to have some variations in the size, location and form of the brain tumor tissues and usually contains any dropsy. Other tissues that contain any dead, bloodshed or shrinkage, can be as abnormality and so abnormal tissues boundaries can be blurred. Second problem is the *MR* images have formed from high number of pixels (for example $256*256*128$), so segmentation problem, has a high computational complexity and needs much memory. This problem can be solve by using *2D* repetitive methods or semi-automatic segmentation helping human knowledge, but will lose much information such as geometry and etc [4].

In the last decades, many methods have been proposed to segment the brain tumor of *MR* images, such as neural networks [13, 14], support vector machine (*SVM*) [15], finite Gaussian mixture model [16], fuzzy *C*-means (*FCM*) [13, 17], knowledge-based methods [18, 19], atlas based method [20], active contour model [21], level set methods [22, 23], and outlier detection [24]. Here, the segmentation task is regarded as a tissue recognition problem, which means using a well-trained model that can determine whether a pixel/ voxel belongs a normal or abnormal tissue.

In general, one could use the supervised classification or the unsupervised clustering methods. Supervised methods [25– 30] may produce good results, however, they require the scrupulous labeling work by doctors or experts. Unsupervised methods [31– 34] could do the segmentation automatically, but sometimes it is difficult to produce a good result. Fully automated methods always cooperate with some human knowledge. This paper has focused on the methods that use the *ANN* as a classifier to segment the brain structures. An earlier method developed by

Magnotta et al [35] used voxel intensity values of the neighboring voxels as the input feature. Their task was to classify the voxels into two classes – being normal or abnormal structure. They designed one ANN for each structure. The input features did not contain any shape representations. This causes the need for large training data sets. On the other hand, voxel intensity values can solve the segmentation problem for the high-resolution MRI they utilized. Recently, Powell et al [36] developed their previous algorithm [35] and added 9 voxel intensity values along the largest gradient, one probabilistic map value, and voxel intensity values along each of the three orthogonal values as the input features. They used high-resolution images the same as [35] for the segmentation of the brain structures.

For the first time, Shen et al [37] used the GMIs for elastic registration of MRI. They utilized them to reflect the underlying anatomy at different scales. They defined similarity measures instead of using a classifier to identify the brain structures. They optimized an objective function to maximize the image similarity. Jabarouti Moghaddam [38] has proposed a two-stage method for the segmentation of the brain structures. In the first stage, he has considered the shape of the structures using the GMIs in different scales along with the neighboring voxels intensity values as the input features and the signed distance function of the structure as the outputs of the ANNs. In each scale, an ANN is designed to approximate the signed distance function of the structure. In the second stage, he has combined the outputs of the ANNs by another ANN to classify the voxels.

In this paper, it is tried to give clear description from brain tissues using Zernike Moments [39], Geometric Moment Invariants [38], Energy, Entropy, Contrast and some other statistic features such as Mean, Median, Variance, Correlation, values of Maximum and Minimum intensity. This paper uses from pixels/voxels coordinates to fill holes between regions and compare matched pixels/voxels with based image pixels/voxels. Based image for each of normal and abnormal tissue is obtained from averaging on all 100 normal and abnormal dataset images separately. feature selection method is used to reduce the feature space too. The method uses from neural network to do this classification. The purpose of this project is to classify the brain tissues to normal and abnormal classes automatically, that saves the radiologist time, increases accuracy and yield of diagnosis.

2. MATERIALS AND METHODS

2.1 Input Data Sets

MR images which been used in this paper are all type of MR images.

2.2 Preprocessing

Images usually contain one or more type of noise and artifact.

In medical images, because of diagnostic and therapeutic applications, this issue is critical. Specially in MR images, inhomogeneous magnetic fields, Patient motions duration imaging times, thermal noise and exist of any metal things in imaging environment, are some reasons that can create noises and artifact, though in most of times, are not very important because of human studies on images ,but these are one of the main causes for computational errors in automatic or semi automatic image analyzing methods and so it is needed to be removed by preprocessing procedures before any analyzing. Here,

preprocessing is equal to remove seeds from images and increase contrast between normal and abnormal brain tissues. The procedure have been used here are Histogram equalization, using Median filter, using Un sharp mask, thresholding and using from Mean filter respectively for each image. In this step, two-dimensional discrete Fourier transform is computed for images. To reduce the noise a 3 by 3 pixel mean filter was implemented. This filtered averaged 9 points thus reducing the noise by 3. Because a single pass of this filter did not seem to provide sufficient noise reduction, the image was passed through the filter a second time (Figure 1).

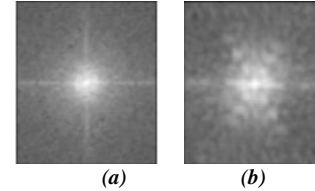


Figure 1: Fourier transform a) abnormal b) normal

As it is obvious at images, the Fourier transform of normal tissue is intensive, whereas it is widespread and amorphous in abnormal images. This difference can be done as one feature named entropy that will be explained at the next sections.

2.3 Image Processing

2.3.1 Feature extraction

The purpose of feature extraction is to reduce the original data set by measuring certain properties, or features, that distinguish one input pattern from another. The extracted features provide the characteristics of the input type to the classifier by considering the description of the relevant properties of the image [42].

The analyzing methods have been done until now used values of voxels intensities [42-51], pixels/voxels coordinate [42, 52, 53] and some other statistic features such as mean, variance or median which have much error in determination process and low accuracy and robustness in classification.

It has been explained about the features that have been used in this paper which are divide to two classes of statistic and non-statistic features. $X(i,j)$ is the value of intensity for location of (i,j) at variation of $\Delta y, \Delta x$ between pixels [42].

2.3.1.1 Statistic features

Mean: The mean is defined as below:

$$\text{Mean (M)} = m: \mathbf{xx} = \frac{1}{x+y} \sum_{i=1}^x \sum_{j=1}^y \mathbf{x}(i, j) \quad (1)$$

Standard deviations: It is square of variance. The variance is defined as below:

$$\text{Variance (V)} = \sigma^2 = \frac{1}{x+y} \sum_{i=1}^x \sum_{j=1}^y (\mathbf{x}(i, j) - m)^2 \quad (2)$$

Entropy: A measure of non uniformity in the image based on the probability of co-occurrence values:

$$Entropy = \sum_{i=1}^N \sum_{j=1}^N \left(\frac{P(i,j)}{R} \right) \log \left(\frac{P(i,j)}{R} \right) \quad (3)$$

Where, N is the number of gray levels, equal to 256 for images in the present study. R is equal to the total number of pixel pairs used for the calculation of texture features in the specified angular direction.

Median: The value that multiplicity of upper values and lower values are equal.

Contrast: A measure of difference moment and is defined as below:

$$Contrast = \sum_{i=1}^N \sum_{j=1}^N (i-j)^2 \left(\frac{P(i,j)}{R} \right) \quad (4)$$

Energy: A measure of homogeneity that can be defined as:

$$Energy = \sum_{i=1}^N \sum_{j=1}^N \left(\frac{P(i,j)}{R} \right)^2 \quad (5)$$

Inverse Difference Moment: A measure of local homogeneity that can be defined as below:

$$I = \sum_{i=1}^N \sum_{j=1}^N \frac{\left[\frac{P(i,j)}{R} \right]}{1+(i-j)^2} \quad (\text{for } i \neq j) \quad (6)$$

Correlation: A measure of linear dependency of brightness and can be defined as below:

$$Correlation = \sum_{i=1}^N \sum_{j=1}^N \frac{\left[\frac{P(i,j)}{R} \right] - \mu_x \mu_y}{\sigma_x \sigma_y} \quad (7)$$

$$\mu_x = \sum_{i=1}^N i \sum_{j=1}^N \left(\frac{P(i,j)}{R} \right), \quad \mu_y = \sum_{i=1}^N j \sum_{j=1}^N \left(\frac{P(i,j)}{R} \right) \quad (8)$$

$$\sigma_x^2 = \sum_{i=1}^N (i - \mu_x)^2 \sum_{j=1}^N \left(\frac{P(i,j)}{R} \right), \quad \sigma_y^2 = \sum_{i=1}^N (j - \mu_y)^2 \sum_{j=1}^N \left(\frac{P(i,j)}{R} \right)$$

In the above expressions, $\mu_x, \mu_y, \sigma_x, \sigma_y$ are the mean and standard deviation values of GCM values accumulated in the x and y directions, respectively.

2.3.1.2 Non statistic features

Geometric moment Invariant

The GMI's include rich geometric properties that represent the underlying anatomical structures and thus help the ANN to distinguish between the voxels are tumor or not.

The GMI's are calculated as follows. Suppose the origin of the coordinate system is shifted to the voxel x. Then, the 3D-regular moments of order (p + q + r) for the membership function $f_{tissue}(x_1, x_2, x_3) = \{image\}$ are defined by:

$$M_{p,q,r} = \iiint_{(x_1)^2 + (x_2)^2 + (x_3)^2 < R^2} (x_1)^p (x_2)^q (x_3)^r f_{tissue}(x_1, x_2, x_3) dx_1 dx_2 dx_3 \quad (9)$$

Where, R is the radius of the spherical neighborhood around the origin. For example for second order moments:

$$I_1 = M_{2,0,0} + M_{0,2,0} + M_{0,0,2} \quad (10)$$

$$I_2 = M_{2,0,0}M_{0,2,0} + M_{2,0,0}M_{0,0,2} + M_{0,2,0}M_{0,0,2} - M_{1,0,1}^2 - M_{1,1,0}^2 - M_{0,1,1}^2$$

$$I_3 = M_{2,0,0}M_{0,2,0}M_{0,0,2}I_1 + 2M_{1,1,0}M_{1,0,1}M_{0,1,1}$$

$$-M_{0,0,2}M_{1,1,0}^2 - M_{0,2,0}M_{1,0,1}^2 - M_{2,0,0}M_{0,1,1}^2$$

Readers for more information can refer to [38, 54].

Zernike moments

Here, It is explained about Zernike moments from [55]. Readers for more information can refer to it.

The angle between the y axis and the axis passing through the center of mass in head's posterior-anterior direction, which is called h_{head} , is computed on the segmented MR image by using moment properties. The formulas related to h_{head} computation are given below. Before computing h_{head} , the center of mass of the segmented head is computed by using:

$$\bar{x} = \frac{1}{N} \sum_{(x,y) \in T} x, \quad \bar{y} = \frac{1}{N} \sum_{(x,y) \in T} y \quad (11)$$

Here, T denotes the head region with pixels having '1' values (the pixels outside T take '0'); x i-th and y are the coordinates of pixels in region T; N is the number of pixels in T; x and y denote the coordinates of the center of mass of region T.

Moments of order (p + q) are given below:

$$m_{p,q} = \sum_{(x,y) \in T} (x - \bar{x})^p \cdot (y - \bar{y})^q \quad (12)$$

Where $m_{p,q}$ represents the central moment of order (p + q) for p, q = 0, 1, 2, ..., m, h_{head} is computed by using Eq(13) Jain, 1989.

$$\theta_{head} = \frac{1}{2} \text{Arctan} \left[\frac{2m_{1,1}}{m_{2,0} + m_{0,2}} \right] \quad (13)$$

Angle h_{head} is used to determine the symmetry axis.

$$y_{sym} = x \cdot \cos(\theta_{head}) + y \cdot \sin(\theta_{head}) \quad (14)$$

Where x and y are the coordinates of the segmented MR image and represents the symmetry axis (line inclined at an angle of h_{head} from the y-axis).

Moments for (p, q) = 0, in Eq.(12), give the numbers of pixels on the left and right hand sides of the symmetry axis in the tissue of the segmented image. In Eq. (17), weighted areas $WA_{L,i}$ and $WA_{R,i}$ are determined as the moments computed for the tissues on either side of the symmetry axis:

$$m_{R,i,0} = \sum_{(x,y) \in Ri} \sum (x - \bar{x})^i \cdot (y - \bar{y})^0 \quad (15)$$

$$m_{L,i,00} = \sum_{(x,y) \in L_i} \sum (x - \bar{x})^u \cdot (y - \bar{y})^v$$

$$m_{T,i,00} = m_{R,i,00} + m_{L,i,00} \quad (16)$$

$$WA_{L,i} = \frac{m_{L,i,00}}{m_{T,i,00}}, \quad WA_{R,i} = \frac{m_{R,i,00}}{m_{T,i,00}} \quad (17)$$

$$WA_i = |WA_{L,i} - WA_{R,i}| \quad (18)$$

where $m_{L,i,00}$ and $m_{R,i,00}$ represent the numbers of the pixels on the left and right hand sides of the symmetry axis in the i -th tissue (T_i) of the segmented image, respectively.

$|WA_{L,i} - WA_{R,i}|$ will be used to determine the tissue with tumor.

2.3.2 Feature selection

Kernel F-score method

First, the *F-score* method is explained and after that, it is explained about the *kernel F-score* method. Readers can refer to [20] for more details.

F-score method is a basic and simple technique that measures the distinguishing between two classes with real values. In *F-score* method, *F-score* values of each feature in dataset are computed according to following equation (Eq. (19)) and then in order to select the features from whole dataset, threshold value is obtained by calculating the average value of *F-scores* of all features. If the *F-score* value of any feature is bigger than threshold value, that feature is added to feature space. Otherwise, that feature is removed from feature space. Given training vectors x_k , $k = 1, \dots, m$, if the number of positive and negative instances are n_+ and n_- , respectively, then the *F-score* of the i -th feature is explained as follows:

$$F(i) = \frac{(\bar{x}_i^{(+)} - \bar{x}_i)^2 + (\bar{x}_i^{(-)} - \bar{x}_i)^2}{\frac{1}{n_+ - 1} \sum_{k=1}^{n_+} (\bar{x}_{ki}^{(+)} - \bar{x}_i)^2 + \frac{1}{n_- - 1} \sum_{k=1}^{n_-} (\bar{x}_{ki}^{(-)} - \bar{x}_i)^2} \quad (19)$$

Where \bar{x}_i , $\bar{x}_i^{(+)}$, $\bar{x}_i^{(-)}$ is the average of the i -th feature of the whole, positive, and negative data sets respectively. $\bar{x}_{ki}^{(+)}$ is the i -th feature of the k -th positive instance and $\bar{x}_{ki}^{(-)}$ is the i -th feature of the k -th negative instance. The numerator shows the discrimination between positive and negative sets, and the denominator defines the one within each of the two sets. The larger *F-score* for one feature means this feature is more discriminative. But a disadvantage of *F-score* method does not take the mutual information between features into account. In the proposed feature selection method, *kernel F-score* feature selection method is provided both to transform from non-linearly separable dataset to linearly separable dataset and to decrease the computation cost of classification algorithm. First of all, input spaces (features) of dataset have been mapped to kernel space using Linear (*Lin*) or Radial Basis Function (*RBF*) kernel functions. In this way, the dimensions of datasets have transformed to high dimensional feature space. After transforming

from input space to kernel space, the *F-score* values of datasets with high dimensional feature space have been calculated using *F-score* formula. And then the mean value of calculated *F-scores* has been computed and also this value is selected as threshold value. If the *F-score* value of any feature in datasets is bigger than threshold value, that feature will be selected. Otherwise, that feature is removed from feature space. Thanks to *KFFS* method, the irrelevant or redundant features are removed from high dimensional input feature space. The cause of using *kernel* functions transforms from non-linearly separable medical dataset to a linearly separable feature space.

2.3.3 Purposed method

purposed method contains 2 steps. In first step, defiant structures are estimated using a neural network and the statistic features that have been explained. These structures are thought be part of tumor or contains tumor.

In second step, finally it is decided about which defiant structures are really tumor or contains tumor using another neural network and non statistic feature (*Geometric moment Invariant*, *Zernike moments*). At end, it has been done some post processing procedures with morphological procedures such as filling and connected components algorithms to connect the probable discrete points which are exist at image. Tumor location is determined by measuring the primary and extremity points coordinates and then compute length, width and height for measuring the volume of tumor. The parts below have explained more about each stage.

2.3.3.1 First stage: finding defiant structures

In this stage, each input feature vector contains all features that are mentioned at the statistic features. At each pixel such as x , the feature vector of $F(x)$ formed from 8 line of vector. In other word $F(x) = [I(x) \ A(x) \ E(x) \ C(x) \ M(x) \ V(x) \ D(x)]$ where $I(x)$, $R(x)$, $A(x)$, $E(x)$, $C(x)$, $M(x)$, $V(x)$, $D(x)$, are Inverse Difference Moment, Entropy, Energy, Contrast, Mean, Standard deviation, Median at the mask with the size of 3 with desired pixel center after passing feature selection stage respectively.

Here, we use from one *MLP* to explain the relationship between inputs and outputs. Different Architectures have been tested and finally selected one neural network with 8 neuron(input features) at input layer, 5 neuron at first hidden layer, 3 neuron at second hidden layer, and one neuron at the output layer. The output features are distance function from tumor structures. This function is subset of defiant functions in description of structures. This function at tumor regions are positive, is zero on the boundary and negative at other areas. At the point that are Adjacent to boundary the absolute values decreases.

The neural network has been trained using back propagation algorithm and training process has been continued until the Mean Square Error (*MSE*) became constant. At this stage is not expected that *MSE* be zero, because have been used from statistic features and know some points that is determined by

network as tumor are not really tumor or contains no tumor. The training process lasts about 7 hours.

2.3.3.2 Second stage: accurate tumor determination

First stage outputs are diverse between different areas. The first stage neural network outputs are merged .this neural network, works such a classifier not such an estimator. The goal of this stage is classifying the image voxels to 2 classes of normal and abnormal.

The input feature vector in this stage contains the non statistic feature (*GMI*s and *Zernike* moments) plus all first stage outputs. In other word, at each pixel such as x , the feature vector of $F(x)$ formed from 4 line of vector. In other word, $H(x)$ can be defined $H(x) = [O(x), Z(x), G(x), N(x)]$ where $O(x)$ is the vector that contains all outputs of first stage, $G(x)$ and $Z(x)$ are the vectors that contains *GMI*s and *Zernike* moments after passing through feature selection stage respectively, and $N(x)$ is the vector that contains voxel coordinates in Cartesian coordinate system. The voxels coordinates helps the network to express better input-output relationship and fill the ruptures to create contiguous results.

The neural network in this stage is *MLP* too. Here like first stage, different architectures tested. and finally one neural network with 19 neuron(input features) at input layer,11 neuron at first hidden layer,5 neuron at second hidden layer, and one neuron at the output layer has been selected. Activation functions are sigmoid at all layers. In this stage, training process lasts about 76 hours. Though this time is much but this process done for just one time and this time is lower in comparison of other similar methods in literatures.

2.3.4 Final processing

In this stage, small holes and unreal pixels is removed by image morphological algorithms. Here, has been used from two image processing morphological algorithms: image filling and connected-component algorithms. image filling is used for filling the holes between network outputs and connected-component used to remove the unreal pixels. In this stage, tumor location is determined by measuring the primary and extremity points coordinates and then compute length, width and height for measuring the volume of tumor.

3. RESULTS

During the classification process of the tumors types, a *MLP* has been used with two hidden layers only. In order to evaluate the classification efficiency, two metrics have been computed: (a) the training performance (i.e. the proportion of cases which are correctly classified in the training process) and (b) the testing performance (i.e. the proportion of cases which are correctly classified in the testing process). Basically, the testing performance provides the final check of the *NN* classification efficiency, and thus is interpreted as the diagnosis accuracy using the neural networks support. Recall that the testing performance, corresponding to the neural networks-based diagnosis accuracy, involves only cases with unknown diagnosis for the neural network classifier. This represents an alternative to traditional

classification performance measures, such as sensitivity, specificity etc. and is directly related to this Artificial Intelligence technique.

Technically, 160cases are randomly selected used for training, 40 cases remaining for testing.

Firstly, notice that a testing performance of 98.2% on average has been obtained (98.22% of cases are correctly classified in the testing process), together with a high training performance equaling 99.1% on average (99.1% of cases are correctly classified in the training process). Thus, the neural networks-based diagnosis accuracy is 98.9% on previously unknown cases, proving a good potential for this methodology. Usually, the training performance is higher than the testing performance, since the latter concerns unknown cases. In this case, the two measures are close enough (difference of less than 1 percentage points only), indicating a low over-learning level, that is a balanced training/testing process. Moreover, the corresponding standard deviations equaling about 1 and 2 percentage points respectively indicate a high stability of the model, especially in the training case. Note that, as training progresses, the training error naturally drops; it is desirable that the testing error should decrease as well as the training error as training progresses. If the difference between the two errors increases too much, this indicates that the network is starting to over-learn the data and thus it is applicable to other datasets anymore.

Secondly, the mean number of hidden processing units (neurons) in the network equals 12 $((5+11+5+3)/2=12)$, with a relative high standard deviation, equaling 3. This means that a two-hidden layer *MLP* with 9 neurons on average is able to provide 98.9% diagnosis accuracy. Moreover, it is possible to build a neural network model with 6 neurons only, that is a simple neural structure, and obtain a good enough accuracy. On the other hand, more than 15 neurons are not necessary to obtain a better classification. Thus, we can conclude that it is possible to have a relative simple network structure (i.e. a small number of hidden neurons), that is a fast *NN* with a very good performance. Recall that an efficient neural computing solution to real-life problems implies the selection of the simplest *NN* architecture with high performance.

Performance measures

All classification result could have an error rate and on occasion will either fail to identify an abnormality, or identify an abnormality which is not present. It is common to describe this error rate by the terms true and false positive and true and false negative as follows [52, 69, 70]:

True Positive (TP): the classification result is positive in the presence of the clinical abnormality.

True Negative (TN): the classification result is negative in the absence of the clinical abnormality.

False Positive (FP): the classification result is positive in the absence of the clinical abnormality.

False Negative (FN): the classification result is negative in the presence of the clinical abnormality.

In this study because of measuring more real and robust results the method has been tested 10 times on all dataset and have computed the Performance measures as below:

$$\text{Sensitivity} = TP / (TP + FN) * 100\% = 347 / (347 + 3) * 100\% = 98.14\%$$

$$\text{Specificity} = \text{TN} / (\text{TN} + \text{FP}) * 100\% = 344 / (344 + 6) * 100\% = 98.28\%$$

$$\text{Accuracy} = (\text{TP} + \text{TN}) / (\text{TP} + \text{TN} + \text{FP} + \text{FN}) * 100 = (347 + 344) / (344 + 347 + 3 + 6) * 100\% = 98.71\%$$

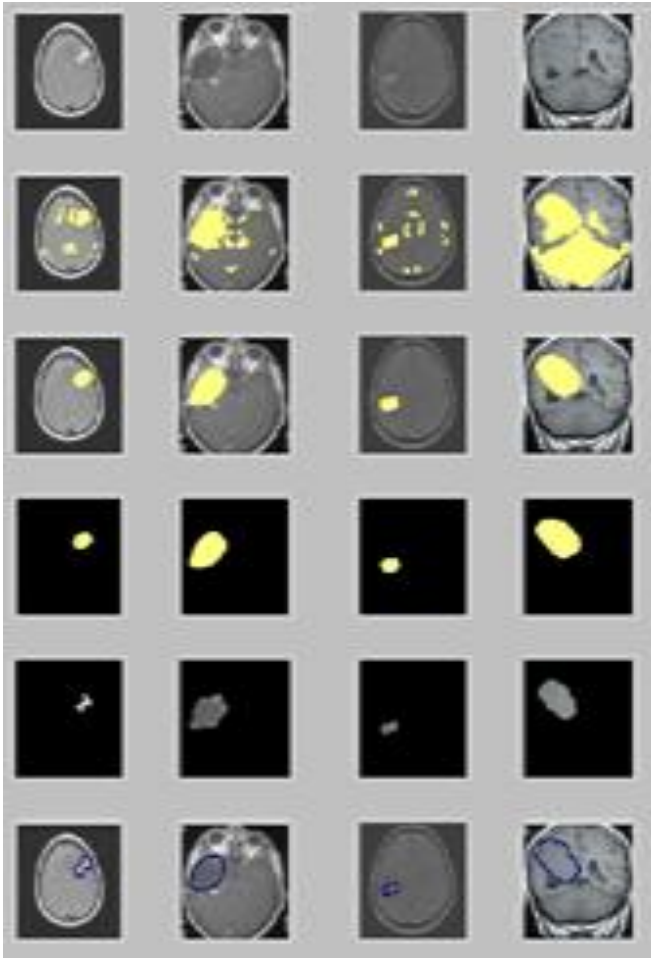


Figure 2: End results for 4case : from upper left to down : original image _ after first stage _ image post processing _after second stage _output image

It has been presented qualitative comparison results of the segmented image too. The performance of the network is derived from the *MSE* value. No further improvement in the *MSE* is observed after epoch 100 as shown in (Fig.3), with a performance measure of 0.01798.

4. . CONCLUSION

Different types of elasticity imaging procedures have recently been described in the medical literature, with clinical applications already developed for the diagnosis of abnormalities. The methodology has been developed in this paper, is based on processing sample images of tumor and normal tissues, enables the exploration and analysis by automatic means of large

quantities data from large number of patients. This provides a method which is an alternative to traditional human-based techniques, and optimally predicts the presence or absence of abnormality by using a noninvasive methodology.

The application of neural networks models in non-invasive abnormality diagnosis, using sample images, represents a promising complementary method, enhancing and supporting the differential diagnosis of normal tissue and abnormalities made by physicians, in real time and with a high degree of accuracy, compared to traditional methods, but much faster.

The results obtained in this project are really good in terms of computational efficiency.

This work, can be justify by its high power, accuracy and yield in detecting each type of abnormalities.

The tasks that can derive from this project, include the integration of features derived from Fractal Analysis which describe Local Texture or Ruggedness in terms of an estimated value called *Hurst Coefficient*. These results are expected to be used in conjunction with Wavelet Multi resolution. Moreover, a classification performance analysis based on *ROC* curves is also needed to complete the study.

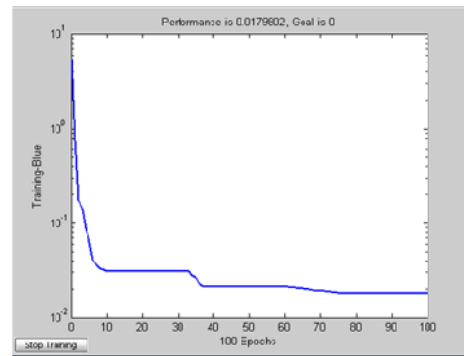


Figure 3: Method performance

5. REFERENCES

- [1] Ashby LS, Troester MM, Shapiro WR “ Central Nervous System Tumors ” Cancer Therapeutics, Vol.1, pp. 475-513, 2006.
- [2] Cruickshank G, “ Tumours of The Brain Surgery ” Oxford, 22, pp.69-72 (2004).
- [3] Doolittle ND, “ State of The Science in Brain Tumor Classification”, Semin Oncol Nurs, vol.20, pp.224- 230 (2004).
- [4] Yangqiu Song Æ Changshui Zhang Æ Jianguo Lee Æ Fei Wang Æ Shiming Xiang Æ Dan Zhang “Semi-supervised discriminative classification with application to tumorous tissues segmentation of MR brain images” Pattern Anal Applic, vol.12, pp. 99–115 (2009).
- [5] Pham DL, Xu C, Prince JL “Current methods in medical image segmentation” Annu Rev Biomed Eng 2:315–337 (2000).
- [6] Liew AWC, Yan H “ Current methods in the automatic tissue segmentation of 3D magnetic resonance brain images” Curr Med Imaging Rev 2(1):91–103 (2006).

- [7] Leemput KV, Maes F, Vandermeulen D, Suetens P “Automated model-based tissue classification of MR images of the brain” *IEEE Trans Med Imaging* 18(10):897–908 (1999).
- [8] Pham D, Prince J “Adaptive fuzzy segmentation of magnetic resonance images” *IEEE Trans Med Imaging* 18(9):737–752 (1999).
- [9] Zhang Y, Brady M, Smith SM “Segmentation of brain MR images through a hidden Markov random field model and the expectation maximization algorithm” *IEEE Trans Med Imaging* 20(1):45–57 (2001).
- [10] Marroquín JL, Vemuri BC, Botello S, Caldero F, Fernandez-Bouzas A “An accurate and efficient Bayesian method for automatic segmentation of brain MRI” *IEEE Trans Med Imaging* 21(8):934–945 (2002).
- [11] Liew AWC, Yan H “An adaptive spatial fuzzy clustering algorithm for 3d MR image segmentation” *IEEE Trans Med Imaging* 22(9):1063–1075 (2003).
- [12] Prastawa M, Gilmore JH, Lin W, Gerig G “Automatic segmentation of neonatal brain MRI” In: *Proceedings of medical image computing and computer-assisted intervention (MICCAI)*. pp 10–17 (2004).
- [13] Hall L, Bensaid A, Clarke L, Velthuizen R, Silbiger M, Bezdek J “A comparison of neural network and fuzzy clustering techniques in segmenting magnetic resonance images of the brain” *IEEE Trans Med Imaging* 3(5):672–682 (1992).
- [14] Sammouda R, Niki N, Nishitani H “A comparison of Hopfield neural network and Boltzmann machine in segmenting MR images of the brain” *IEEE Trans Nucl Sci* 43(6):3361–3369 (1996).
- [15] Zhou J, Chan KL, Chongand VFH, Krishnan SM “Extraction of brain tumor from MR images using one-class support vector machine” In: *Proceedings of 27th annual international conference of the IEEE Engineering in Medicine and Biology Society (EMBS)*. pp 6411–6414 (2005).
- [16] Moon N, Bullitt E, Leemput KV, Gerig G “Automatic brain and tumor segmentation” In: *Proceedings of 5th international conference on medical image computing and computer-assisted intervention (MICCAI)*. pp 372–379 (2002).
- [17] Shen S, Sandham W, Granat M, Sterr A “MRI fuzzy segmentation of brain tissue using neighborhood attraction with neural-network optimization” *IEEE Trans Med Imaging* 9(3):459–467 (2005).
- [18] Li C, Goldgof D, Hall L “Knowledge-based classification and tissue labeling of MR images of human brain” *IEEE Trans Med Imaging* 12(4):740–750 (1993).
- [19] Clark M, Hall L, Goldgof D, Velthuizen R, Murtagh F, Silbiger M “Automatic tumor segmentation using knowledge-based techniques” *IEEE Trans Med Imaging* 17(2):187–201 (1998).
- [20] Cuadra M, Pollo C, Bardera A, Cuisenaire O, Villemure JG, Thiran JP “Atlas-based segmentation of pathological MR brain images using a model of lesion growth” *IEEE Trans Med Imaging* 23(10):1301–1314 (2004).
- [21] Zhu Y, Yan Z “Computerized tumor boundary detection using a hopfield neural network” *IEEE Trans Med Imaging* 16(1):55–67 (1997).
- [22] Droske M, Meyer B, Rumpf M, Schaller C “An adaptive level set method for medical image segmentation” In: *Proceedings of 17th international conference information processing in medical imaging (IPMI)*. Davis, CA, USA, pp 416–422 (2001).
- [23] Lefohn AE, Cates JE, Whitaker RT “Interactive, GPUbased level sets for 3D segmentation” In: *Proceedings of medical image computing and computer-assisted intervention (MICCAI)*. Springer, Montreal, QC, Canada, pp 564–572 (2003).
- [24] Prastawa M, Bullitt E, Ho S, Gerig G “Robust estimation for brain tumor segmentation” In: *Proceedings of medical image computing and computer-assisted intervention (MICCAI)*, pp 10–17 (2004).
- [25] Guemur Y “Combining discriminant models with new multi-class SVMs” *Pattern Anal Appl* 5(2):168–179 (2002).
- [26] Tortorella F “Reducing the classification cost of support vector classifiers through an ROC-based reject rule” *Pattern Anal Appl* 7(2):128–143 (2004).
- [27] Debnath R, Takahide N, Takahashi H “A decision based one-against-one method for multi-class support vector machine” *Pattern Anal Appl* 7(2):164–175 (2004).
- [28] Sa’anchez JS, Mollineda RA, Sotoca JM “An analysis of how training data complexity affects the nearest neighbor classifiers” *Pattern Anal Appl* 10(3):189–201 (2007).
- [29] Abe S “Sparse least squares support vector training in the reduced empirical feature space” *Pattern Anal Appl* 10(3):203–214 (2007)
- [30] Herrero JR, Navarro JJ “Exploiting computer resources for fast nearest neighbor classification” *Pattern Anal Appl* 10(4):265–275 (2007).
- [31] Tyree EW, Long JA “A monte carlo evaluation of the moving method, k-means and two self-organising neural networks” *Pattern Anal Appl* 1(2):79–90 (1998).
- [32] Chou CH, Su MC, Lai E “A new cluster validity measure and its application to image compression” *Pattern Anal Appl* 7(2):205–220 (2004).
- [33] Frigui H “Unsupervised learning of arbitrarily shaped clusters using ensembles of gaussian models” *Pattern Anal Appl* 8(1-2):32–49 (2005).
- [34] Omran MGH, Salman A, Engelbrecht AP “Dynamic clustering using particle swarm optimization with application in image segmentation” *Pattern Anal Appl* 8(4):332–344 (2006).
- [35] Magnotta, V.A., Heckel, D., Andreasen, N.C., Cizadlo, T., Corson, P.W., Ehrhardt, J.C., Yuh, W.T.: *Measurement of brain Structures with Artificial neural Network: two and three-dimensional applications*. *Radiology* 211(3), 781–790 (1999).
- [36] Powell, S., Magnotta, V.A., Johnson, H., Jammalamadaka, V.K., Prerson, R., Anderasen, N.C.: *Registration and Machine Learning-based Automated Segmentation of Subcortical and Cerebellar brain Structures*. *NeuroImage* 39, 238–247 (2008).
- [37] Shen, D., Davatzikos, D.: *HAMMER: Hierarchical Attribute Matching Mechanism for elastic Registration*. *IEEE Trans. Med.* 21(11), 1421–1439 (2002).
- [38] Mostafa Jabarouti Moghaddam and Hamid Soltanian-Zadeh, “Automatic Segmentation of Brain Structures Using Geometric Moment Invariants and Artificial Neural Networks” *IPMI 2009, LNCS 5636*, pp. 326–337 (2009).
- [39] Chakeres DW, Schmalbrock P “*Fundamentals of Magnetic Resonance Imaging*” Williams & Wilkins, Baltimore (1992).
- [40] Buxton RB “*Introduction to Functional Magnetic Resonance Imaging-Principles and Techniques*”. Cambridge University Press (2002).
- [41] Alan Wee, Chung Liew, Hong Yan, “Current Methods in the Automatic Tissue Segmentation of 3D Magnetic Resonance Brain Images,” *Current Medical Imaging Reviews*, Vol.2, pp.1-13 (2006).
- [42] H. Selvaraj1, S. Thamarai Selvi2, D. Selvathi3, L. Gewali1, “Brain MRI Slices Classification Using Least Squares Support Vector Machine” *IC-MED*, Vol.1, No. 1, Issue 1, Page 21 of 33 (2007).
- [43] Karteek Popuria, Dana Cobzasb, Martin Jagersandb, Sirish L. Shaha and Albert Murthac, “3D Variational Brain Tumor Segmentation on a Clustered Feature Set”, *SPIE*, 1-4 (2009).
- [44] Marcel Prastawa a, Elizabeth Bullitt c, Sean Ho a, Guido Gerig, “A Brain Tumor Segmentation Framework Based on Outlier Detection” *Medical Image Analysis*, 1-9 (2004).
- [45] Jiayin Zhou, Vincent Chong, Tuan-Kay Lim, Jing Huang, “MRI Tumor Segmentation for Nasopharyngeal Carcinoma Using Knowledge-based Fuzzy Clustering” *International Journal of Information Technology* Vol. 8, No. 2 (September 2002).
- [46] Jason J. Corso, Member, IEEE, Eitan Sharon, Shishir Dube, Suzie El-Saden, Usha Sinha, and Alan Yuille, “Efficient Multilevel Brain Tumor Segmentation with Integrated Bayesian Model Classification” *IEEE Transactions on Medical Imaging*, pp.1-7 (2007).
- [47] Dzung L. Pham, Chenyang XU, and Jerry L. Prince2 “Current methods in Medical Image Segmentation1”, *Biomed. Eng.*, vol.2 pp.315-337 (2000).
- [48] <http://documents.wolfram.com>

- [49] Dzung L. Pham, Chenyang Xu, Jerry L. Prince; "A Survey of Current Methods in Medical Medical Image Segmentation" Technical Report JHU / ECE 99-01, Department of Electrical and Computer Engineering, The Johns Hopkins University, Baltimore MD 21218 (1998).
- [50] 1Nathan Moon, 2Elizabeth Bullitt, 4Koen van Leemput, and 1;3Guido Gerig, " Automatic Brain and Tumor Segmentation", MICCAI2002,LNCS2488(I) pp. 372-379
- [51] Rajeev Ratan A, Sanjay Sharma B, S. K. SharmaC, "Brain Tumor Detection Based on Multi-Parameter MRI Image Analysis", ICGST-GVIP Journal, ISSN 1687-398X, Vol.9,Issu (III),(June 2009).
- [52] Carlos A. Parra, Khan Iftekharuddin and Robert Kozma, "Automated Brain Data Segmentation and Pattern Recognition Using ANN" , Computational Intelligence, Robotics and Autonomous Systems (CIRAS 03), (December2003).
- [53] Alan Wee-Chung Liew¹ and Hong Yan, "Current Methods in the Automatic Tissue Segmentation of 3D Magnetic Resonance Brain Images" Current Medical Imaging Reviews, vol.2, 1-13 (2006).
- [54] Lo, C.H., Don, H.S.: 3-D Moment Forms: Their Construction and Application to Object Identification and Positioning. IEEE Trans. on Pattern Analysis and Machine Intelligence 11(10), 1053–1064 (1989).
- [55] Zafer Iscan, Zümray Dokur, Tamer Ölmez "Tumor detection by using Zernike moments on segmented magnetic resonance brain images" Expert Systems with Applications 37, 2540–2549 (2010).
- [56] Kemal Polat, Salih Gunes, "A New Feature Selection Method on Classification of Medical Datasets:Kernel F-score Feature Selection" , Expert Systems with Applications, vol.36 pp.10367–10373 (2009).
- [57] Alirezaie, J.; Jernagan, M.E.; Nahmias, C. " Automatic Segmentation of Cerebral MR Images Using Artificial Neural Networks" Nuclear Science Symposium (1996). Conference Record IEEE , Vol.3, pp.2-9 (1996). vol.3, pp. 1777 -1781 (Nov. 1996).
- [58] Alirezaie, J.; Jernagan, M.E.; Nahmias, C.; Neural Network Based Segmentation of Magnetic Resonance Images of the Brain" Nuclear Science Symposium and Medical Imaging Conference Record, (1995), IEEE , Vol.3 .pp.21-28 (1995) vol.3 pp. 1397 -1401 (Oct 1995).
- [59] Sammouda, R.; Niki, N.; Nishitani, H. "Neural Networks Based Segmentation of Magnetic Resonance Images" Nuclear Science Symposium and Medical Imaging Conference(1994), IEEE Conference Record, Vol.4 (1994) vol.4, 1827 -1831 ,(30 Oct , 5 Nov 1994).
- [60] Porter, R.; Hockett, S.; Canagarajah, C.N "Optimal Feature Extraction for the Segmentation of Medical Image"s. Image Processing and Its Applications (1997)., Sixth International Conference on , Vol.2 , pp.14-17 vol.2 ,pp .814 -818 (Jul 1997).
- [61] R.O. Duda, P.E. Hart, and D.G. Stork, "Pattern Classification", Wiley, 2nd edition (2001).
- [62] J. A. Freeman and D. M. Skapura, "Neural Networks, Algorithms, Applications and Programming Tech-niques", Addison-Wesley Publishing Company (2002).
- [63] C.M Bishop, "Neural Networks for Pattern Recognition", Oxford U.K: Clarendon (1995).
- [64] S. Haykin, "Neural networks: A comprehensive Foundation", 2nd ed. Englewood Cliffs, NJ: Prentice Hall (1999).
- [65] F. M. Ham and I. Kostanic, "Principle of Neurocomputing for Science and Engineering" Tata McGraw-Hill publishing company Limited, New Delhi (2002).
- [66] F. Belloir, A. Fache, and A. Billat, "A General Approach to Construct RBF Net Based Classifier", Proceedings of the 7th European Symposium on Artificial Neural Network, pp. 399 404 (1999).
- [67] Y. S. Hwang and S. Y. Bang, "An Efficient Method to Construct a Radial Basis Function Neural Network Classifier", Neural Networks, vol. 10, no. 8, pp. 1495-1503 (1997).
- [68] C. J. C. Burges, "A tutorial on Support Vector Machines for Pattern Recognition", Data Mining and Knowledge Discovery,vol.2,no.2, pp.121–167 (1998).
- [69] R.M. Nishikawa, M.L. Giger, K. Doi, C.J. Vyborny, and R.A. Schmidt, "Computer Aided Detection of Clustered Microcalcifications in Digital Mammograms," Med. Biol. Eng. Comp. Vol. 33, pp. 174-178 (1995).
- [70] S. Theodoridis and K. Koutroumbas, "Pattern Recognition", Academic Press, San Diego, (1999).
- [71] N.G. Raouf, Naguib, H. A. M. Sakim, M.S. Lakshmi, V. Wadehra, T. W. J. Lennard, J. Bhatavdekar, and G. V. Sherbat, "DNA Ploidy and Cell Cycle Distribution of Breast Cancer Aspirate Cells Measured by Image Cytometry and Analyzed by Artificial Neural Networks for their Prognostic Significance," IEEE Transaction on Information Technology in Biomedicine. Vol. 3, No. 1 (1999).

Amir Ehsan Lashkari is MSC Student of the Department of Bioelectrical Engineering, University of Tehran, Tehran, Iran,Asia. He received his BS from the Faculty of Bioelectric, Iran University of Isfahan in 2009 .His research interests are in: **Digital Image Processing, Neural Networks, Pattern Recognition, Intelligent Systems, Machine Vision, Fuzzy Logic, Chaos and Fractal Phenomena, Digital Design, Artificial Intelligent, Digital Signal Processing, Network and Path Planning, Multiple Valued Function, Programmable Device.**

He is top Student of university and he has published 3 books until now. The project he has done are: A Neural Network based Method for Brain Abnormality Detection in MR Images Using Gabor Wavelets, 2009/A Neural Network-Based Method for Brain Abnormality Detection in MR Images Using Zernike Moments and Geometric Moment Invariants, 2009/Full Automatic Micro Calcification Detection in Mammogram Images Using Artificial Neural Network and Gabor Wavelets, 2010/Automatic Gabor Face Detection by Neural Net work, 2010/Automatic Brain Tissue segmentation In MR Images by Neural Net work, 2009/Automatic Defect Detection in Steel Sheet in MOBARAKE STEEL FACTORY, Isfahan,2008/Automatic Label Reading in Cars, 2008/Automatic Growth Prediction of Tumors, By Inteligent Methods , 2008/Automatic Chromosome Obvolute in Microscopic Image By fuzzy Logic, 2009/Automatic Separation Chromosome Obvolute in Microscopic Image By fuzzy Logic, 2009/Parameter Optimization in Factory, 2010/Chaos and Fractal Signal Prediction In Biological System, 2010 and etc.